Electronic Supplementary Information

A H_2O_2-free electrochemical peptide biosensor based on Au@Pt bimetallic nanorods for highly sensitive sensing of Matrix Metalloproteinase 2

Xiaoxue Xi[a], Meiqi Wen[a], Shihao Song [a], Junlun Zhu[a], Wei Wen[a,*], Xiuhua Zhang[a], Shengfu Wang[a,*]

[a]State Key Laboratory of Biocatalysis and Enzyme Engineering, Ministry of Education Key Laboratory for the Synthesis and Application of Organic Functional Molecules and College of Chemistry and Chemical Engineering, Hubei University, Wuhan 430062, PR China

***Corresponding Authors:**
Telephone: +86-27-88662747; Fax: +86-27-88663043.
E-mail: Wei Wen, Email: wenwei@hubu.edu.cn; Shengfu Wang, Email: wangsf@hubu.edu.cn.

MATERIALS AND METHODS

Materials. Sodium borohydride ($NaBH_4$), chloroauric acid ($HAuCl_4.3H_2O$), chloroplatinic acid ($H_2PtCl_6.6H_2O$), cetyltrimethylammonium bromide (CTAB), silver ($AgNO_3$), ascorbic acid (AA), H_2SO_4, 3,3′,5,5′-tetramethylbenzidine (TMB), N,N-Dimethylformamide (DMF), hydrogen peroxide (H_2O_2), disodium hydrogen phosphate (Na_2HPO_4), monopotassium phosphate (KH_2PO_4), sodium chloride (NaCl), N-(3-Dimethylaminopropy1)-N-ethylcarbodiimide (EDC), N-Hydroxysuccinimide (NHS), chitosan (CS), Trimethyl-amino methane (Tris), calcium (Ⅱ) chloride dihydrate ($CaCl_2.2H_2O$), iron (III) chloride hexahydrate ($FeCl_3.6H_2O$), copper (Ⅱ) chloride dihydrate ($CuCl_2.2H_2O$), PSA, glucose, bovine serum albumin (BSA), thrombin (TB), arginine, glutamate were purposed from Aladdin Regen Co, Ltd (shanghai, China). Graphene quantum dots were purposed from Xianfeng nanomaterials technology Co, Ltd (Nanjing, China).

The MMP-2 specific peptide (-KGRVGLPGC-) was purchased from Sangon Biotech (Shanghai, China) Co., Ltd. The MMP-2 was purposed from Yiqiao Shenzhou technology Co., Ltd (Beijing, China). The activating agent 4-aminophenylmercuric acetate (APMA) was purchased from Jiemei gene medicine technology Co., Ltd. (Shanghai, China).

The Ultra-pure water (18.25MΩ cm) in the experiment came from the Aquapro water purification system. Phosphate buffered solution (PBS) (10mM, pH=7.4) serving as working buffer throughout the experiment. TCNB buffer (0.05% Brij 35, 150 mM NaCl, 50 mM Tris, 10 mM $CaCl_2$, pH=7.5).

Characteristics. The morphological features of Au NRs and Au@Pt nanorods were explored by Transmission electron microscopy (TEM) images (100 KV HITACHI H-7000F and 300 KV FEI Tecnai G2F30), and scanning electron microscopy (SEM) images (Sigma 500), X-ray photoelectron spectroscopy (XPS) measurements (ESCALAB 250Xi) was used to investigate the chemical valence of the element. X-ray diffraction (XRD) (BRUCK, D8 ADVANCE) was conducted to study the crystal structure of Au@Pt nanorods. The measurement of Ultraviolet-visible (UV-Vis) absorption spectra throughout the experiment was carried out by UV-Vis spectrophotometer (UV-2700, Shimadzu, Japan and UH4150 Tokyo Japan).

Synthesis of nanoparticles. Noble metal nanomaterials have attracted many interests in recent years due to their excellent catalytic activity and wide application value, especially gold and platinum, and the methods of directional design and regulation of the size of nanoparticles have been widely studied by many groups[1-3].

The Au NRs and Au@Pt nanorods were synthesized according to a classic seed-mediated growth method with a little modification[4]. The details of the synthesis process are presented as follows: before starting, all of the glass instruments were soaked in aqua regia (V_{HCl} : V_{HNO3}=3:1) for 20 min, rinsed with ultrapure water for several times and dried in an infrared oven.

(Ⅰ). Synthesis of Au NRs : Firstly, Au seeds were obtained via a chemical reduction method with $HAuCl_4$ and $NaBH_4$ as raw materials: 3.75 mL CTAB (0.1M) solution was mixed with 50 μL $HAuCl_4$ (24 mM) and diluted with water to 4.7 mL, 0.3 mL ice-cold $NaBH_4$ (0.01M) was added quickly accompanied with stirring magnetically. After stirring vigorously for 3 minutes, the solution was kept undisturbed for 2-5 h, and then the seed solution was obtained with a dark brown color. Then the Au NRs were prepared by a seed-mediated growth method containing 60 mL CTAB (0.1 M), 1.224 mL $HAuCl_4$ (24 mM), 1.2 mL H_2SO_4 (0.5 M), 0.6 mL $AgNO_3$(10 mM), 480 μL AA (0.1 M), 150 μL seed solutions. The mixed solutions were stirring vigorously for 3 minutes, and kept it undisturbed at room temperature for 12 h. After that, the Au NRs wee purified by centrifugation (10,000 rpm 9 min) twice. The precipitates were collected and re-dispersed in deionized water with the same volume.

(Ⅱ). Synthesis of Au@Pt nanorods: 20 mL above Au NRs solutions were diluted to 40 mL with deionized water, then 2 mM H_2PtCl_4 and 0.1 M ascorbic acid (AA) ($AA/PtCl_4^{2-}$=5:2) were added to above solutions rapidly, heating it for 30 min in the 30 ℃ water. And keep it undisturbed for 14 h until the color changed from wind-red to dark-gray, which suggesting the successful synthesis of Au@Pt nanorods. Finally 1.0 mL CTAB was added to stop the reaction and prevent the aggregation of it. Then the solution was centrifuged (9000 rpm, 10 min) and concentrated for twice to remove excess impurities, the obtained solutions were kept at 4 ℃ with a brown bottle for further use. The TEM images and Zeta potential of the same batch synthesized Au@Pt nanorods but characterized at intervals of several months were obtained to investigate the stability of material. As shown in Fig. 1 and Fig. S2, after months of storage, the morphology and effective

diameter of Au@Pt nanorods have no obvious changes, and there was no serious aggregation happened either. Besides, the Zeta potential was also performed to exhibit the stability of the material, as depicted in Fig. S8, the Zeta potential also exhibited no obvious changes after storage of several months. Therefore, the Au@Pt nanorods exhibited a satisfactory stability, which can keep their catalytic activity and morphology without serious aggregation under 4 ℃ storage for several months.

Preparation of CS-GQDs-COOH. The nanocomposites of CS-GQDs were prepared as follows: 1% Chitosan (CS) solution was prepared by dissolving CS into acetic acid solution in a glass reactor fitted with a magnetic stirrer.

And then 1 mg/mL GQDs aqueous solutions were mixed with 1% Chitosan (CS) solution, whirl and ultrasonic to get homogeneous solutions with a concentration of 0.8 mg/mL. The obtained CS-GQDs nanocomposites were stored at 4 ℃ for further use.

Preparation of peptide-based electrochemical biosensor. The electrochemical peptide biosensor was fabricated on a GCE electrode. Firstly, the pretreatment process of the GCE is also important, the GCE electrode was polished with 0.05 μm α-Al_2O_3 polishing powder, followed by successive sonication with pure water, ethanol and pure water for 5 min, respectively. After blowing dry with nitrogen, 10 μL CS-QDs-COOH (0.8 mg/mL) mixed solution was dropped onto the surface of the electrode. After drying at room temperature, EDC (0.4 M) and NHS (0.1 M) solutions were mixed together and incubated with CS-QDs/GCE for 30 min to activate the -COOH group on the electrode. Secondly, the MMP-2 specifically recognized peptides are self-assembled on the chitosan-graphene quantum dots (CS-GQDs-COOH) modified GCE electrode through an amide reaction. After washing with PBS buffer and drying at room temperature, the specific recognizing peptide (20 μM) of MMP-2 was added and incubated at room temperature for 1.5 h to prepare peptide/CS-QDs/GCE through amide reaction, and the electrode was rinsed with PBS buffer thoroughly to remove the non-specific. Then 1% BSA was used and incubated with above modified electrode for 30 min to block the excess active sites, and then the electrode was rinsed absolutely with PBS buffer and ultrapure water to remove the excess BSA molecule. Thirdly, the twice concentrated Au@Pt nanorods are immobilized subsequently through layer-by-layer assembly at room temperature over night via Au-S bond. After each incubation step, the electrode was washed thoroughly with PBS buffer and ultrapure water to avoid the possible non-

specific absorption.

At last, the Au@Pt nanorods can catalyze signal molecules (i.e., TMB) efficiently only with dissolved O_2 in the solutions and generate an intensive electrochemical signal, after adding target MMP-2 to the system, a sharply decline signals were observed. After each assembly, the electrode was rinsed absolutely with PBS solutions to remove possible non-specific adsorbed substances.

Electrochemical detection of MMP-2. Different concentrations of MMP-2 were prepared with TCNB buffer solutions (50 mM tris, 10 mM $CaCl_2$,150 mM NaCl, 0.05 % Brij 35), the MMP-2 was first activated with APMA according to the specification provided by the manufacturer, 100 μL MMP-2 (200 ng/mL) in TCNB buffer was mixed with 10 μL APMA (10 mM) and incubated at 37 ℃ for 1 h. After that, the activated MMP-2 was diluted into different concentrations with TCNB buffer and the peptide-based electrochemical biosensor was immersed into 100 μL MMP-2 for 1 h at 37 ℃, the DPV signal measurement was performed in 3.0 mL PBS buffer solution (PH=7.4, 10 mM) containing 100 μL TMB (10 mM), the concentration of MMP-2 was quantified by a decrease DPV response value ($\Delta I = I_n - I_0$), where I_n and I_0 were the DPV response intensity of the peptide-based biosensor before and after reacted with MMP-2, respectively.

The discussion of the possible catalytic mechanism of Au@Pt nanorods. As we know that Au@Pt nanorods exhibited intrinsic peroxidase-like and oxidase-like activity, which have been investigated by previous researchers[4]. And in our experiment, the TMB can be oxidized only with dissolved O_2 due to the excellent oxidase-like activity of Au@Pt nanorods. It has been reported in many literatures that Pt is the super catalyst for the oxygen reduction reaction (ORR) and H_2O_2 reduction in electrocatalytic process[5-7]. The reaction pathways can be described by the following two equations for O_2 and H_2O_2 as electron acceptors, respectively[4]:

$$O_2 + 4H^+ + 4e^- = 2H_2O \ (\Phi^\theta = +1.23\ V) \qquad (1)$$

$$H_2O_2 + 2H^+ + 2e^- = 2H_2O \ (\Phi^\theta = +1.77\ V) \qquad (2)$$

In electrochemistry, the electrons are provided by applied voltages whereas the electrons herein come from the organic substrates. The oxidation of TMB by oxygen or by H_2O_2 is believed to go through a similar pathway to the electrochemical reductions and is described in equation (3) and (4) with the substrate of TMB. The DPV response current decreased sharply and quickly after

saturation with N_2 of the substrate solution, which means the decline of the reaction rate of TMB oxidation, and the DPV current response quickly return to previous strength after saturation with O_2 of the substrate solution (Fig. 2d). The results indicating that the dissolved oxygen is the electron acceptors for the oxidation in the absence of H_2O_2 and further verify the effective oxidase-like activity of Au@Pt nanorods. Moreover, the mechanism of oxidase-like nanozyme has been investigated by many researchers, a lot of experiments have been conducted and proved that the oxidase-like activity of nanozyme originates from their catalytic ability for activation of dissolved O_2 to generate $^1O_2$ and $O_2^{\cdot-}$ in the TMB oxidation reaction[8-10]. So we infer that the possible Au@Pt nanorods oxidase catalytic mechanism may also rely to the generation of $^1O_2$ and $O_2^{\cdot-}$ in the TMB oxidation reaction with dissolved O_2, and which need to be investigated in detail in the later work.

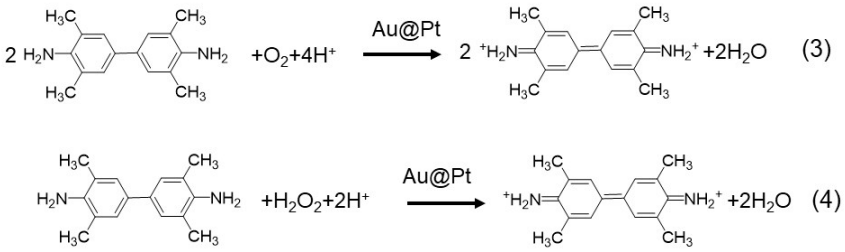

Supplementary results

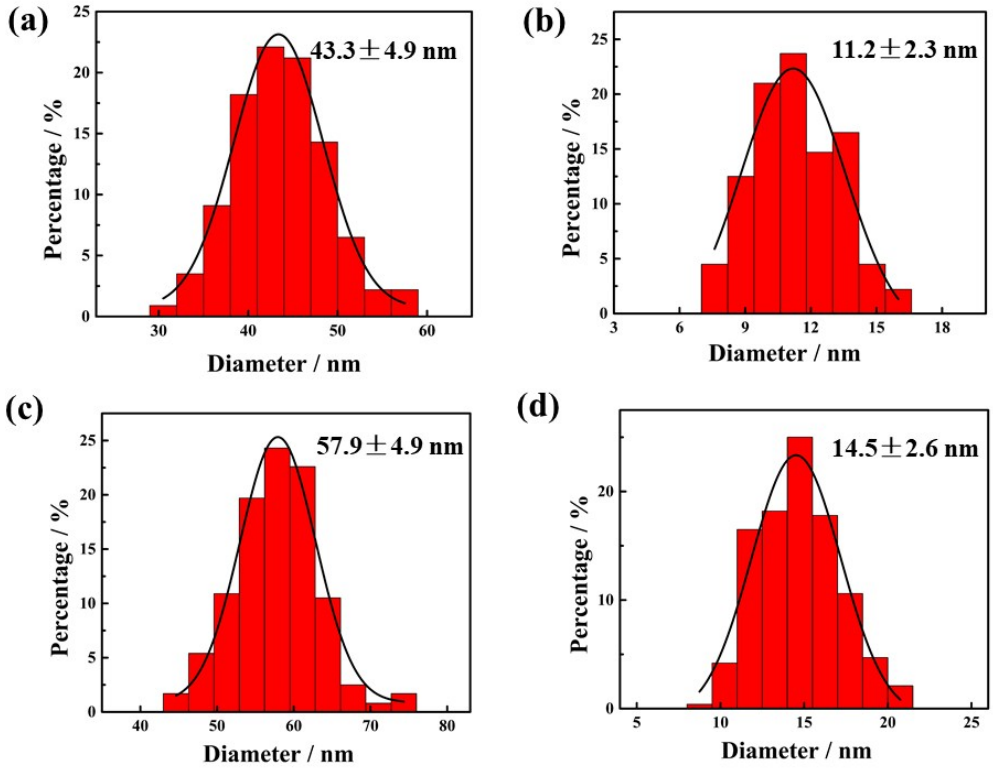

Fig. S1 The size of AuNRs and Au@Pt nanorods was counted by Nano Measurer: the length distribution diagram of the AuNRs (a) and Au@Pt (c); the width distribution diagram of the AuNRs (b) and Au@Pt (d).

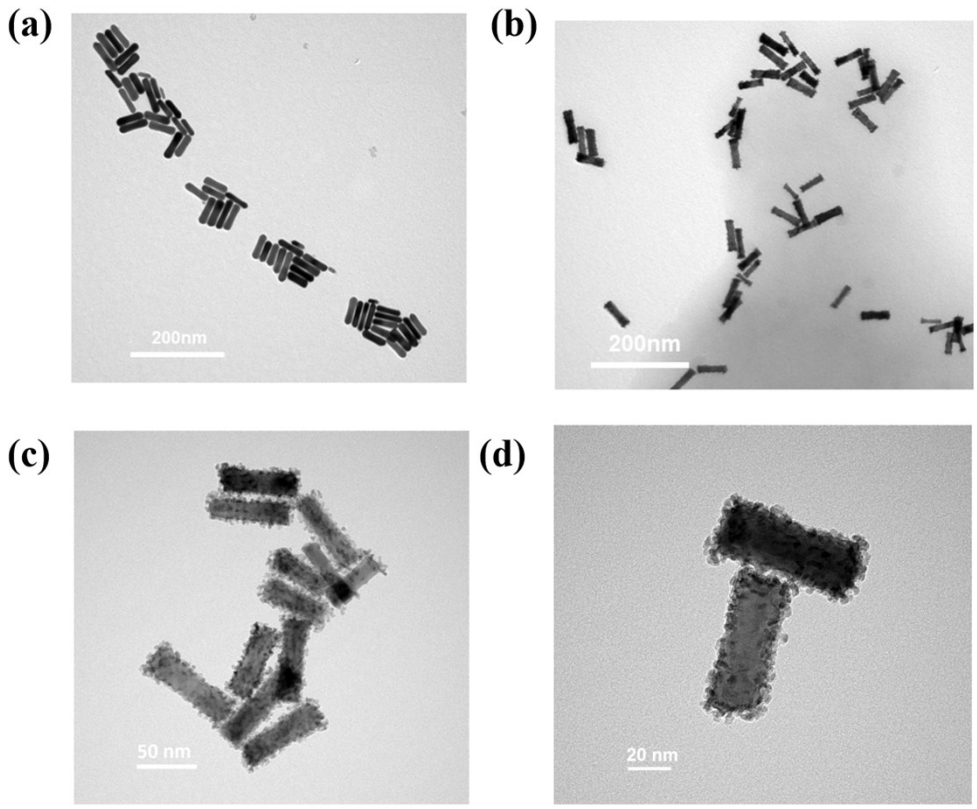

Fig. S2 The TEM images of Au NRs (a), and Au@Pt nanorods with various scales: 200 nm (b); 50 nm (c); 20 nm (d).

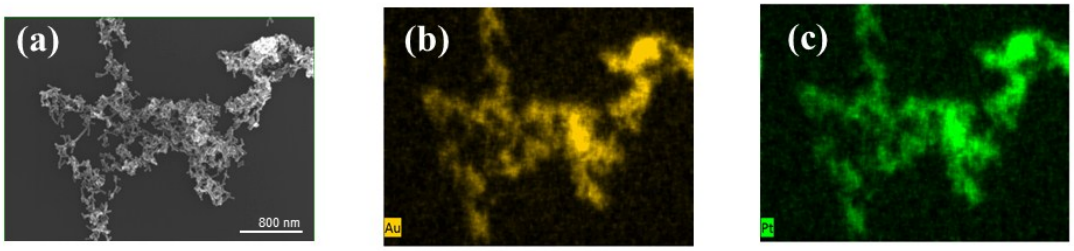

Fig. S3 (a) The SEM images of Au@Pt nanorods; (b-c) EDS element mapping of Au@Pt nanorods.

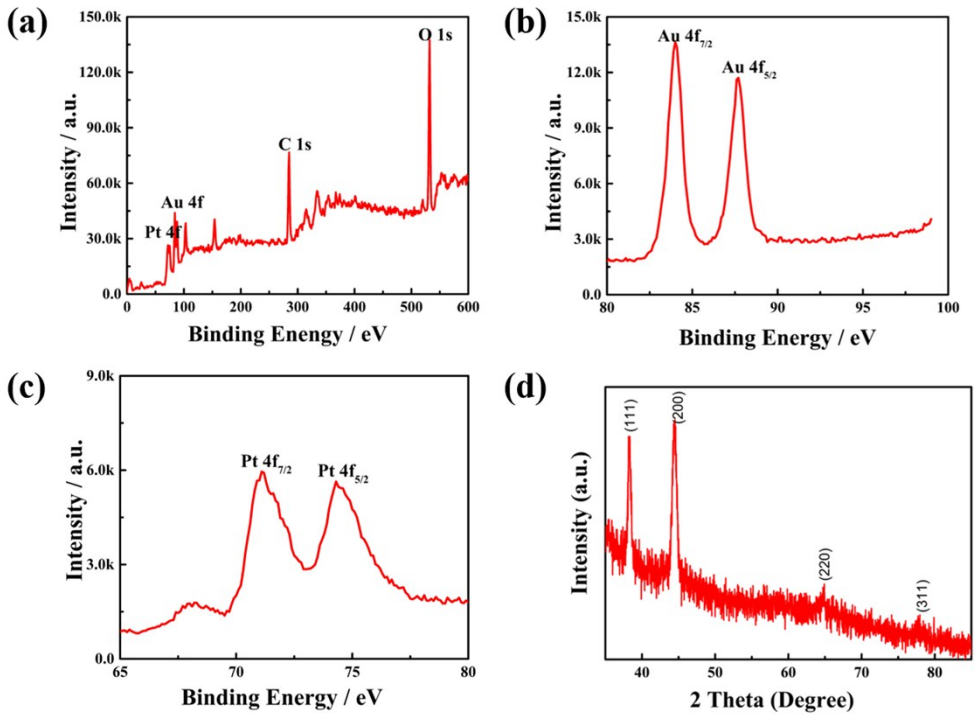

Fig. S4 The high-resolution XPS spectrum of Au@Pt nanorods: full survey spectrum (a); Au 4f (b); Pt 4f (c); and XRD image of Au@Pt nanorods (d).

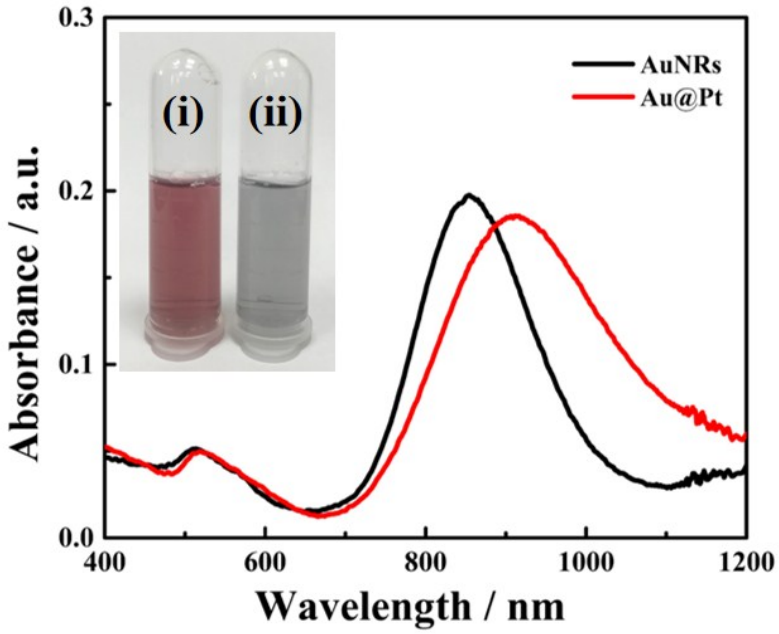

Fig. S5 The UV-Vis absorption spectrum of AuNRs (black line) and Au@Pt nanorods (red line), inset were corresponding colour pictures of Au NRs (ⅰ) and Au@Pt nanorods (ⅱ).

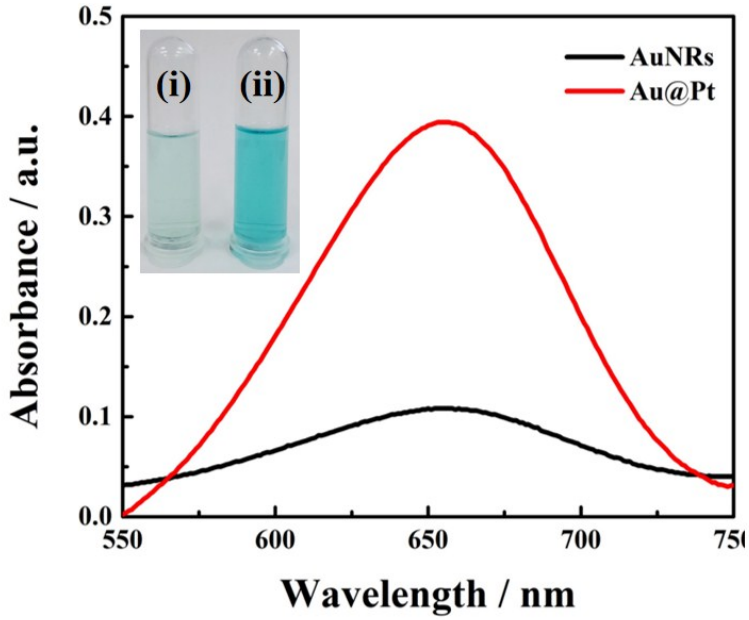

Fig. S6 The absorption spectra with AuNRs and Au@Pt as catalyst in the TMB-O_2 system, inset showed the corresponding final color of different reaction systems (ⅰ)AuNRs+TMB+ NaAc-HAc; (ⅱ) Au@Pt nanorods+TMB+NaAc-HAc. Reaction condition: NaAc-HAc buffer (0.1 M, 2.8 mL), Au NRs solution (100 μL, twice concentrated), Au@Pt nanorods solution (100 μL, twice concentrated), TMB solution (10 mM, 100 μL). The total volume of the reaction solution is 3.0 mL.

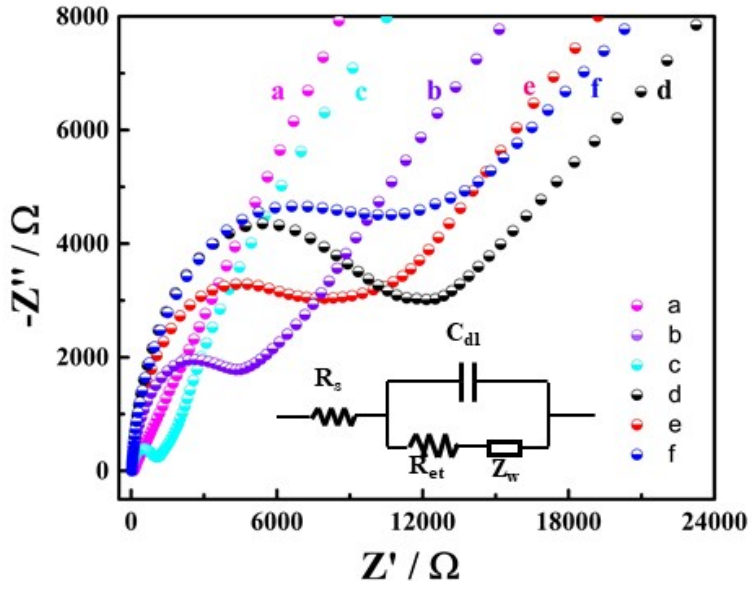

Fig. S7 EIS of the stepwise modified electrodes in 5 mM $[Fe(CN)_6]^{3-/4-}$ containing 0.1 M KCl: (a) bare GCE, (b) GCE/CS-GQDs, (c) GCE/CS-GQDs/pep, (d) GCE/CS-GQDs/ Pep/BSA, (e) GCE/CS-GQDs/pep/BSA/Au@Pt, (f) GCE/CS-GQDs/pep/BSA/Au@Pt/ MMP-2;

Electrochemical impedance spectroscopy (EIS) Characterization：

The stepwise assembly processes for the constructed biosensor were monitored by electrochemical impedance spectroscopy (EIS) in 0.1 M KCl containing 5 mM $[Fe(CN)_6]^{4-/3-}$ as a redox probe. The diameter of the simulated semicircle is equivalent to the electron-transfer resistance (Ret). As depicted in Fig. S7, the bare GCE electrode exhibited a quite small impedance, nearly exhibited a straight line (curve a), which illustrated the excellent electrical conductivity to facilitate the electron-transfer process. The R_{et} increased significantly due to the poor electron-transfer conductivity of chitosan when CS-GQDs-COOH was assembled onto the surface of GCE electrode (curve b). After assembling polypeptide on the CS-GQDs-COOH/GCE surface (curve c), a sharply decrease R_{et} was observed because the positively charged peptide can promote the electron-transfer due to the electrostatic attraction between negatively charged $[Fe(CN)_6]^{4-/3-}$ redox probe and polypeptide[11]. Following the bovine serum albumin (BSA) was introduced to block the excess active sites and hinder the electron-transfer process between GCE and $[Fe(CN)_6]^{4-/3-}$

solution (curve d). Then the R_{et} decreased remarkably after the modification of Au@Pt nanorods on the polypeptide owing to the satisfied electroconductibility of bimetallic synergistic effect (curve e). Finally an increased Ret was obtained after incubation with MMP-2, which can be ascribed to the remove of abundant Au@Pt nanorods from the GCE surface (curve f).

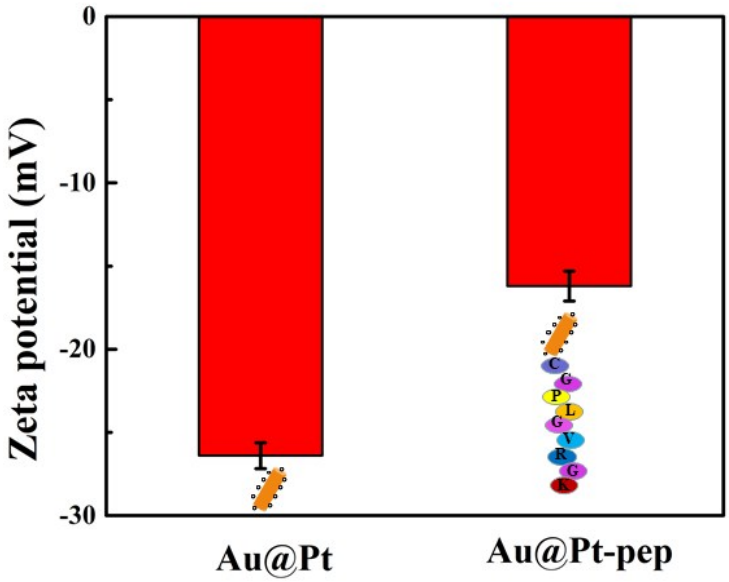

Fig. S8 The Zeta potential of Au@Pt nanorods and Au@Pt-peptide conjugates.

Zeta potential analysis:

Au@Pt nanorods were incubated with peptide (20 μM) stirring and rotating over night, and centrifuged to remove excess uncombined peptide (10000 r/min, 10 min). The obtained compounds were prepared for zeta potential analysis. From the zeta potential results we can observe that the Au@Pt nanorods are negatively charged, and after combining with the positively charged polypeptide, the charges are significantly reduced, which further proved that the successful conjugate of Au@Pt nanorods and peptide through Au-S bond.

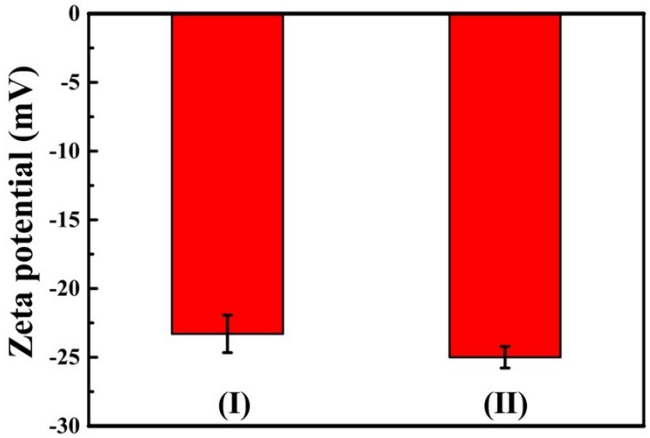

Fig. S9 The Zeta potential of Au@Pt nanorods synthesized with the same batch, characterized before (Ⅰ) and after (Ⅱ) one month.

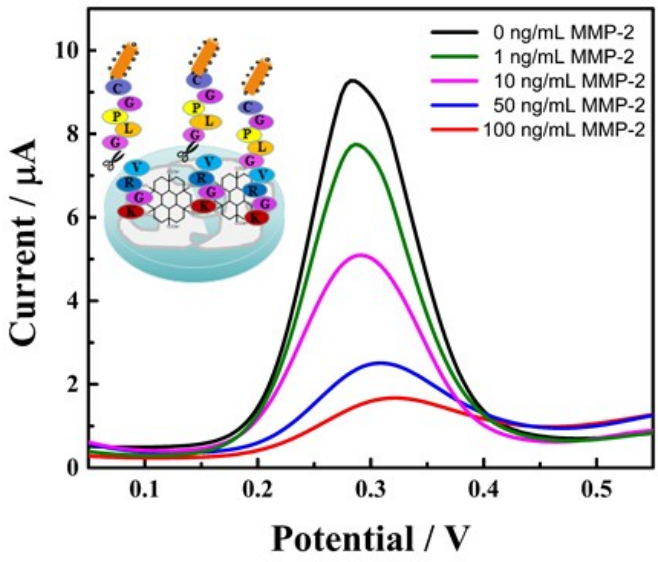

Fig. S10 DPV current responses of the electrochemical peptide biosensor with different concentrations of MMP-2.

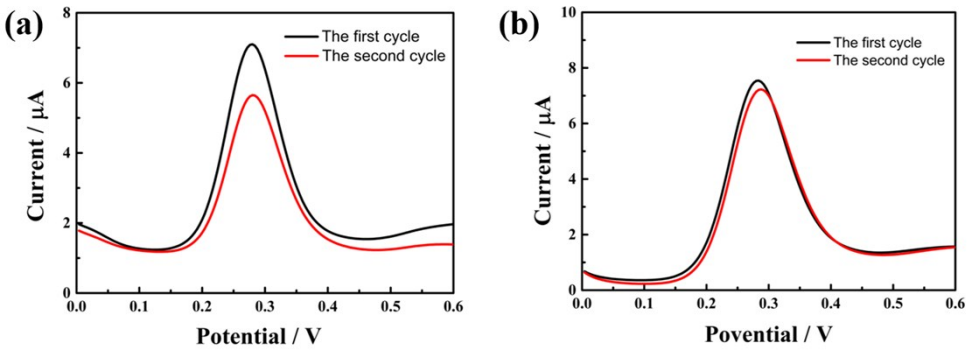

Fig. S11 The DPV current comparison from two rounds of scanning with H_2O_2 (a) and dissolved O_2 (b) involved reaction systems, respectively.

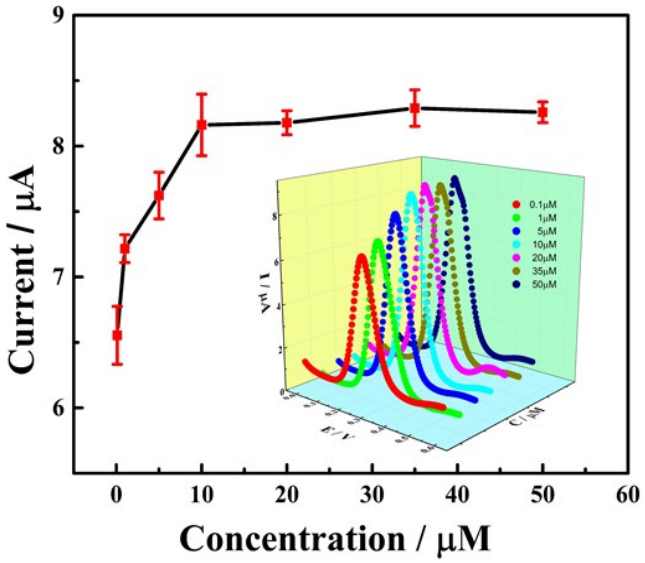

Fig. S12 The optimization of different experimental parameters of the electrochemical response of the biosensor: the concentration of peptide (0.1 μM, 1 μM, 5 μM, 10 μM, 20 μM, 35 μM, 50 μM). (Error bars represent the standard deviations of the three experiments.)

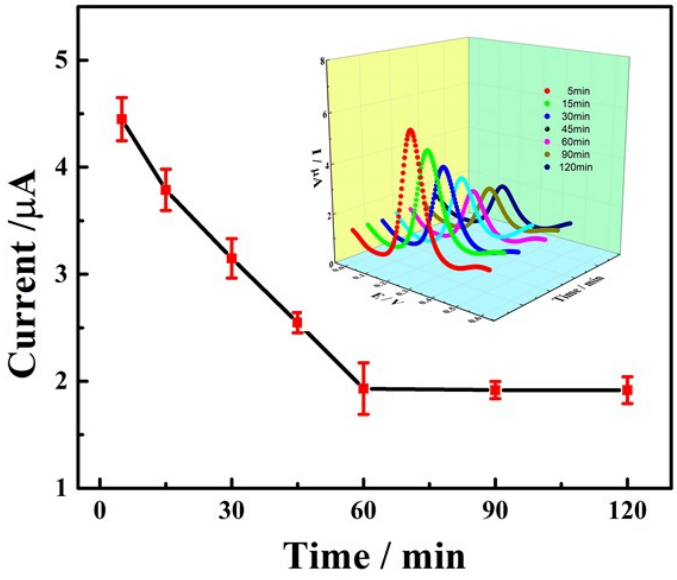

Fig. S13 The optimization of different experimental parameters of the electrochemical response of the biosensor: the incubation time of MMP-2 (5 min, 15min, 30min, 45 min, 60 min, 90 min, 120 min).

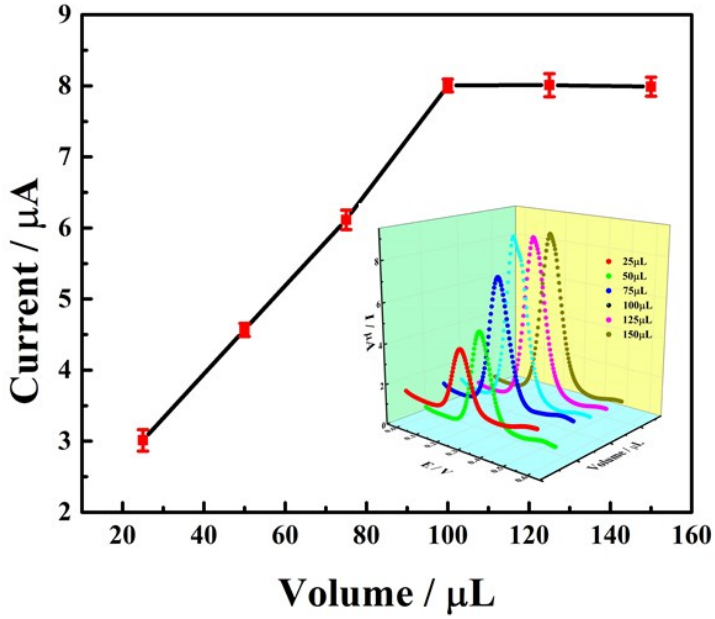

Fig. S14 The optimization of different experimental parameters of the electrochemical response of the biosensor: the volume of TMB (10 mM) of working solution (25 μL, 50 μL, 75 μL, 100 μL, 125 μL, 150 μL).

Table S1. Comparison of different methods for sensitive detection of MMP-2

Detection method	Linear range	Detection limit	Ref.
Electrochemical	1 pg mL^{-1}-1 μg mL^{-1}	0.4 pg mL^{-1}	12
Fluorescence	14.4-144 ng mL^{-1}	3.6 ng mL^{-1}	13
Electrochemical	0.5 pg mL^{-1}-50 ng mL^{-1}	0.15 pg mL^{-1}	14
Electrochemical	0.1 pg mL^{-1}-20 ng mL^{-1}	0.03 pg mL^{-1}	15
Electrochemical	1-200 ng mL^{-1}	0.3 ng mL^{-1}	16
Chemiluminescence	10-300 ng mL^{-1}	5 ng mL^{-1}	17
Electrochemical	0.5-100 ng mL^{-1}	0.18 ng mL^{-1}	This work

Table S2. Recovery test of the electrochemical sensor for MMP-2 in human serum samples

Human serum sample	Add (ng/mL)	Found (ng/mL)	Recovery (%)	RSD(n=3) (%)
1	0.8	0.769	96.1	2.3
2	20	20.87	104.4	4.8
3	80	79.22	99.0	1.2

Reference

1. Ataee-Esfahani, Y. Nemoto, L. Wang, Y. Yamauchi, *Chem. Commun.,* 2011, **47**, 3885-3887.

2. B. Jiang, C.L. Li, J. Tang, T. Takei, Y. Ide, J. Henzie, S. Tominaka, Y. Yamauchi, *Angew. Chem. Int. Ed.,* 2016, **55**, 10037-10041.

3. C.L. Li, H.B. Tan, J.J. Lin, X.L. Luo, S.P. Wang, J. You, Y.M. Kang, Y. Bando, Y. Yamauchi, J. Kim, *Nano Today.,* 2018, **21**, 91-105.

4. W.W. He, Y. Liu, J.J. Yuan, X.C. Wu, X.N. Hu, K. Zhang, J.B. Liu, C.Y. Chen, Y.L. Ji, Y.T. Guo, *Biomaterials.*, 2011, **32**, 1139-1147.

5. N.M. Markovic, H.A. Gasteiger, B.N. Grgur, P.N. Ross, *J Electroanal Chem.,* 1999, **467**, 157e63.

6. J. Zhang, K. Sasaki, E. Sutter, R.R. Adzic, *Science.,* 2007, **315**, 220e2.

7. L. Cai, H.Y. Chen, *Sens Actuators B*., 1999, **55**, 14e8.

8. H.H. Deng, X.L. Lin, Y.H. Liu, K.L. Li, Q.Q. Zhuang, H.P. Peng, A.L. Liu, X.H. Xia, W. Chen, *Nanoscale.,* 2017, **9**, 10292-10300.

9. Y.X. Zhuang, X.D. Zhang, Q.M. Chen, S.Q. Li, H.Y. Cao, Y.M. Huang, *Mater. Sci. Eng. C.,* 2019, **94**, 858-866.

10. H.J. Cheng, S.C. Lin, F. Muhammad, Y.W. Lin, H. Wei, *ACS Sensors.,* 2016, **1**, 1336-1343.

11. C.X. Li, W.S. Lu, M. Zhu, B. Tang, *Anal. Chem*., 2017, **89**, 1098-1106.

12. H.Q. Wang, Z.F. Ma, H.L. Han. *Bioelectrochemistry.*, 2019, **130**, 107324.

13. W. Cheng, Y.L. Chen, F. Yan, L. Ding, S.J. Ding, H.X. Ju, Y.B. Yin, *Chem. Commun.,* 2011, **47**, 2877-2879.

14. D. Wang, Y.L. Yuan, Y.N. Zheng, Y.Q. Chai, R. Yuan, *Chem. Commun.,* 2016, **52**, 5943-5945.

15. B.B. Kou, Y.Q. Chai, Y.L. Yuan, R. Yuan, *Anal. Chem.,* 2017, **89**, 9383-9387.

16. H.F. Xu, H.Z. Ye, L.S. Yu, Y.W. Chi, X.X. Liu, G.N. Chen, *Anal. Methods*., 2015, **7**, 5371-5374.

17. H.F. Gao, Q. Dang, S.Q. Xia, Y. Zhao, H.L. Q, Q. Gao, C.X. Zhang, *Sens Actuators B Chem*., 2017, **253**, 69-76.